


Article

# A Comparative Study of Poly(Azure A) Film-Modified Disposable Electrodes for Electrocatalytic Oxidation of H<sub>2</sub>O<sub>2</sub>: Effect of Doping Anion

Jerónimo Agrisuelas <sup>†</sup>, María-Isabel González-Sánchez, Beatriz Gómez-Monedero and Edelmira Valero \* 

Department of Physical Chemistry, School of Industrial Engineers, University of Castilla-La Mancha, Campus Universitario s/n, 02071 Albacete, Spain; Jeronimo.Agrisuelas@uv.es (J.A.);

MIsabel.Gonzalez@uclm.es (M.-I.G.-S.); Beatriz.Gomez@uclm.es (B.G.-M.)

\* Correspondence: Edelmira.Valero@uclm.es; Tel.: +34-967-599-200

<sup>†</sup> Present address: Department of Physical Chemistry, Faculty of Chemistry, University of Valencia, C/Dr. Moliner 50, 46100 Burjassot, Spain.

Received: 8 November 2017; Accepted: 3 January 2018; Published: 6 January 2018

**Abstract:** In the present paper, poly(azure A) (PAA) films were electrosynthesized in the presence of different doping anions on disposable screen-printed carbon electrodes (SPCEs). The anions used included inorganic monoatomic (chloride and fluoride), inorganic polyatomic (nitrate and sulfate) and organic polyatomic (dodecyl sulfate, DS) species. The coated electrodes thus obtained were characterized by electrochemical techniques and SEM. They showed improved electrocatalytic activities towards hydrogen peroxide oxidation compared to that of a bare SPCE. In particular, the insertion of DS anions inside PAA films provided a special sensitivity to the electrocatalysis of H<sub>2</sub>O<sub>2</sub>, which endowed these electrodes with promising analytical features for H<sub>2</sub>O<sub>2</sub> quantification. We obtained a wide linear response for H<sub>2</sub>O<sub>2</sub> within a range of 5 μM to 3 mM and a limit of detection of 1.43 ± 0.10 μM (signal-to-noise ratio of 3). Furthermore, sensitivity was 72.4 ± 0.49 nA·μM<sup>-1</sup>·cm<sup>-2</sup> at a relatively low electrocatalytic oxidation overpotential of 0.5 V vs. Ag. The applicability of this boosted system was tested by the analysis of H<sub>2</sub>O<sub>2</sub> in commercial samples of a hair lightener and an antiseptic and was corroborated by spectrophotometric methods.

**Keywords:** conducting polymers; poly(azure A); sodium dodecyl sulfate; electrochemical sensor; disposable screen-printed electrodes; hydrogen peroxide

## 1. Introduction

Hydrogen peroxide has been traditionally electrocatalyzed and detected using platinum-based electrodes [1–3] since this metal is a good catalyst for H<sub>2</sub>O<sub>2</sub> decomposition. However, due to its high cost, recycling platinum from waste screen-printed electrodes for the development of new sensors has recently been proposed [4]. The oxidation or reduction of H<sub>2</sub>O<sub>2</sub> on other typical electrodes can be limited by a slow electron transfer rate and high over potentials [5]. Moreover, enzyme-based electrochemical biosensors have a relatively high cost and unstable activities [6]. For these reasons, the search of new materials to solve these shortcomings while presenting similar electroanalytical properties is of paramount importance.

Conducting polymers (CPs) are an appealing approach for electrocatalytic applications given their special characteristics, such as cost-effectiveness, facile synthesis, stability, reproducibility and good sensitivity [7–10]. The electrochemical and conducting properties of CPs depend largely on the electrosynthesis procedure [11–14]. During this process, the polymeric structure and doping agents are fixed in CPs, which confer their special characteristics. Among doping agents, the insertion of electrolytes seems to be one of the most cost-effective options [15].

Among the several strategies developed to reduce costs in the field of electroanalysis, screen-printing is a suitable and simple technique for the mass production of disposable electrodes and design of (bio)sensors [16]. Nowadays, the use of screen-printed electrodes (SPEs) is increasingly extending since they combine several advantages, such as versatility, cost-effective manufacture, minimum analysis volume while avoiding the tedious polishing of solid electrodes and offering the possibility of in situ analysis [17–20]. As far as we know, disposable SPEs modified with organic CPs are still commercially limited, although a number of companies can offer customized solutions.

The electropolymerization of azines and derivatives (e.g., neutral red, azure A or methylene blue) provides an important class of CPs with numerous applications in the sensors field [3,21]. The resulting polymer has two kinds of electroactive double bonds: one between two adjacent monomer molecules and the other within the heterocyclic ring with the participation, in both, of anions and protons for the charge balance [22,23]. Nonetheless, research on SPEs modified by azine-derivative polymers is scarce [24–27].

As a more economical alternative to Pt electrodes, the aim of the present paper was to compare the electroactivity and electrocatalytic oxidation of  $H_2O_2$  driven by disposable screen-printed carbon electrodes (SPCEs) modified by Azure A polymers (PAA). Several PAA films were electrosynthesized under identical experimental conditions, but in different electrolyte solutions including inorganic monoatomic anions (chloride and fluoride), inorganic polyatomic anions (nitrate and sulfate), and an organic polyatomic anion (dodecyl sulfate, DS). The data obtained and their interpretation will be of great interest for extending the use of this type of polymers on disposable electrodes and improving the electrosynthesis of noteworthy films on SPCEs for future sensing applications.

## 2. Materials and Methods

### 2.1. Chemicals and Solutions

L-Ascorbic acid (sodium salt), azure A (80%), caffeine, citric acid (trisodium salt), L-dehydroascorbic acid (DHA), D(+)-glucose,  $H_2O_2$  (35%),  $K_2SO_4$  (99%),  $Ru(NH_3)_6Cl_3$  (98%) and sodium dodecyl sulfate (SDS, 95%) were purchased from Sigma-Aldrich (Madrid, Spain). Reagents for the spectrophotometric measurement of  $H_2O_2$  by the classical xylenol orange method (ammonium iron (II) sulfate hexahydrate, D(–)-sorbitol and xylenol orange (disodium salt)) [28] were also acquired from Sigma-Aldrich. KF and  $KNO_3$  (99.5%) were obtained from Fluka (Darmstadt, Germany). KCl (99.5%) and ethanol (99.9%) were purchased from Scharlau (Barcelona, Spain).  $KH_2PO_4$  (99.5%) and  $K_2HPO_4$  (99%) were sourced from Merck (Darmstadt, Germany). Potassium ferrocyanide (99.95%) was obtained from Probus (Badalona, Spain) and  $H_2SO_4$  (95–98%) was obtained from Panreac (Castellar del Vallès, Spain). The samples of hair lightener (stated composition: water, alcohol denat, Chamomilla recutita flower extract, hydrogen peroxide, parfum, phosphoric acid, amyl cinnamal, coumarin, linalool) and antiseptic (3% hydrogen peroxide) were purchased from a local supermarket. All the reagents were used as received with no further purification. Stock solutions of samples were prepared by appropriate dilutions in 0.1 M potassium phosphate buffer (pH 7).

Solutions were prepared with demineralized water purified by a Milli-Q purification system (18.2 M $\Omega$ -cm) (Millipore Corp, Bedford, MA, USA). For the polymerization solutions, 0.02 M of the appropriate electrolyte was prepared in aqueous solution. Subsequently, 0.1 M phosphate buffer solution (pH 7) was prepared from  $K_2HPO_4$  and  $KH_2PO_4$  to be used as the supporting electrolyte for electrochemical measurements.

### 2.2. Electrosynthesis of PAA Films

PAA films were electrogenerated on the surface of the working electrode (carbon) of disposable SPCEs (DRP-150, DropSens, Oviedo, Spain) with an AUTOLAB potentiostat-galvanostat set-up (PGSTAT204) controlled by the NOVA 2.0 software package. The geometrical area of these electrodes was 12.6 mm<sup>2</sup>, which was used to calculate current densities. A Pt foil (area = 0.49 cm<sup>2</sup>) was used as

the counter electrode during PAA electrosynthesis to keep the counter electrode integrity of the SPCE. The potentials used herein were consistently based on the Ag pseudo-reference electrode of SPCEs.

The electrosynthesis solution consisted of a dissolution of  $1 \text{ mg}\cdot\text{mL}^{-1}$  of azure A in 0.02 M either KCl, KF,  $\text{KNO}_3$ ,  $\text{K}_2\text{SO}_4$  or SDS. To this end, twenty voltammetry cycles were carried out between  $-0.25 \text{ V}$  and  $1 \text{ V}$  at  $10 \text{ mV}\cdot\text{s}^{-1}$  (initial potential,  $E_i = 0.5 \text{ V}$ ). The modified disposable electrodes thus obtained were named as PAA(anion used in electrosynthesis), i.e., PAA(Cl), PAA(F), PAA( $\text{NO}_3$ ), PAA( $\text{SO}_4$ ) and PAA(DS). After deposition, the modified SPCEs were rinsed with abundant ethanol to remove the residual monomers adsorbed on PAA films. They were subsequently cleaned with abundant double-distilled water to eliminate residual ethanol. Finally, dry electrodes were stored in airtight containers while not in use.

Modified SPCEs were characterized by cyclic voltammetry in 0.1 M phosphate buffer. For this purpose, the Pt and Ag electrodes from SPCEs were used as counter and reference electrodes, respectively. Cyclic voltammeteries were performed from  $0.5 \text{ V}$  to  $-0.7 \text{ V}$ , and vice versa, unless otherwise specified.

### 2.3. Electrochemical Impedance Spectroscopy (EIS)

EIS of the modified SPCEs was carried out at  $0.12 \text{ V}$  in 5 mM potassium ferrocyanide and 0.1 M KCl aqueous solution, by means of an AUTOLAB potentiostat-galvanostat set-up (PGSTAT128N) equipped with a frequency response analyzer (FRA) module. Modified working electrodes were polarized for 60 s. A sinusoidal small amplitude potential perturbation ( $5 \text{ mV rms}$ ) was subsequently superimposed between 65 kHz and 10 mHz, with five points per decade. The experimental data were fitted to the equivalent circuit by means of the EIS Spectrum Analyzer (v 1.0, Physico-Chemical Research Institute, Belarusian State University, Minsk, Republic of Belarus) [29].

### 2.4. Electrocatalytic Oxidation of $\text{H}_2\text{O}_2$

Cyclic voltammetry and amperometry were used to compare the electrocatalytic capabilities towards  $\text{H}_2\text{O}_2$  oxidation of the PAA films obtained in 0.1 M phosphate buffer (pH 7). Buffered solutions (10 mL) remained under constant magnetic agitation at room temperature. Calibration was obtained by successive  $\text{H}_2\text{O}_2$  additions and by measuring the current intensity after stabilization.

### 2.5. Scanning Electron Microscopy Images

The surface morphology of all the PAA films electrosynthesized herein was examined by scanning electron microscope (SEM) (mod. Jeol LTD., JSM-6469LV, Akishima, Japan) at an acceleration voltage of 20 kV. It was necessary to cover samples with a gold-platinum thin film of about 2 nm by sputtering to avoid any electric charge effect, which could affect image acquisition. A K-575X Emitech Sputter Coater from Quorum Technologies (Quorum Technologies Ltd., East Grinstead, West Sussex, UK) was used for this purpose.

### 2.6. Spectroscopy

Spectrophotometric measurements were taken in a UV/Vis Perkin-Elmer Lambda 35 (Perkin Elmer Instruments, Waltham, MA, USA) spectrophotometer. Hydrogen peroxide concentration in the samples was measured by the conventional xylenol orange method at 550 nm following the instructions given by the supplier.

## 3. Results and Discussion

### 3.1. Electrosynthesis of PAA Films on SPCEs

Doping ions used in the synthesis solution as the counter-charge to maintain the electroneutrality principle during macromolecular structure formation of CPs define the size and shape of the hydrated cavities inside polymeric films and, as a result, strongly affect their electrochemical properties [30–32].

As PAA films are unresponsive to the cation in the electroynthesis solution [27], we focused on the effect of three kinds of anions in the electroynthesis solution, namely: (i) inorganic monoatomic anions, e.g., chloride and fluoride; (ii) inorganic polyatomic anions, e.g., nitrate and sulfate; and (iii) one organic polyatomic anion, dodecyl sulfate.

Figure 1 shows the voltammetric response of PAA films electrodeposited on the surface of SPCEs using  $1 \text{ mg}\cdot\text{mL}^{-1}$  of azure A in  $0.02 \text{ M}$  KF (Figure 1A),  $\text{K}_2\text{SO}_4$  (Figure 1B) and SDS aqueous solution (Figure 1C). The electroynthesis of PAA, using either  $0.02 \text{ M}$  KCl or  $\text{KNO}_3$  showed very similar profiles to the results observed for KF or  $\text{K}_2\text{SO}_4$ , respectively (data in Figure S1 of the Supplementary Material). In all the electroynthesis solutions, azure A was radicalized by electrochemical oxidation above  $0.5 \text{ V}$  [33]. Radical cations thus formed connections to one other by creating stable covalent bonds between monomers (amine-based intermonomeric links). Polymerization progress was evidenced by the increase in current observed between  $0.5 \text{ V}$  and  $-0.25 \text{ V}$ , which is directly related with the amount of amine-based intermonomeric links formed during the polymerization process [34]. As seen in Figure 1, the achieved voltammetric currents increased as the anions in solution became molecularly more complex.

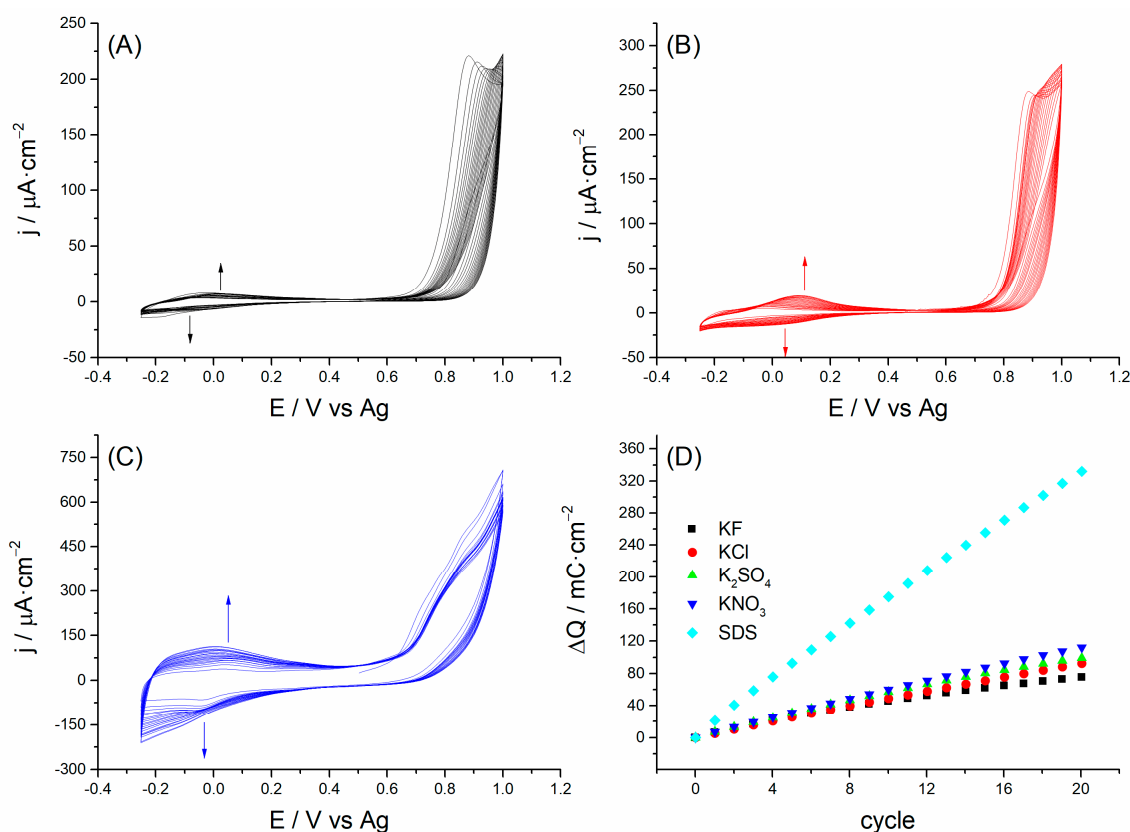


**Figure 1.** Polarization curves of  $1 \text{ mg}\cdot\text{mL}^{-1}$  azure A in  $0.02 \text{ M}$  KF (A),  $\text{K}_2\text{SO}_4$  (B) and SDS (C) aqueous solutions at a scan rate of  $10 \text{ mV}\cdot\text{s}^{-1}$  between  $-0.25 \text{ V}$  and  $1 \text{ V}$ . The voltammetry cycle starts at  $0.5 \text{ V}$ . (D) Charge accumulation during the electrochemical reactions of PAA(anion) electroynthesis calculated from the voltammetric cycles shown in (A–C) and Figure S1.

Integrating these currents over the experimental time allowed us to calculate the consumed charge during the electrode reactions, which is proportional to the amount of electroactive PAA deposited on SPCEs. Figure 1D shows the accumulated charge after each voltammetric cycle for the electroynthesis of the different PAA films. Two different kinds of evolution of charge can be distinguished.

On the one hand, for both inorganic monoatomic and polyatomic anions, the charge increase was almost linear up to the tenth cycle and then curved. The formation of two layers with a different

morphology and structure in the electrosynthesized CP might be the reason [35]. The internal layer in contact with the surface electrode would be the electroactive part of film, while the external layer in contact with the bulk solution would act as a diffusion membrane that hinders the ionic exchange between the electroactive layer and the solution.

On the other hand, the charge consumed during PAA electrosynthesis in SDS solutions was significantly the highest one and maintained a near linear increase, at least during the first 20 cycles. In this case, SDS would favor the polymerization process and might be responsible for this more pronounced linear increase since this anionic surfactant concentrates azure A monomers into SDS micelles [36], thus enhancing the electron transfer between the surface of the PAA film and the monomers in solution [32,37,38].

### 3.2. Electrochemical Response

Figure 2 shows the electrochemical response of a bare SPCE and the synthesized PAA films in 0.1 M phosphate buffer (pH 7). As can be observed, the bare SPCE showed no relevant electroactivity around  $-0.3$  V (Figure 2A, black line). In contrast, PAA films exhibited good electroactivity as revealed by a well-defined pair of electrochemical peaks (Figure 2A,B). Notably, the charge consumed during a cyclic voltammogram of PAA(DS) films (Figure 2B, blue line) was between two-fold and five-fold higher compared to the charge consumed for the other PAA(anion) films. These results corroborated the findings mentioned in the preceding paragraph, and indicate that PAA(DS) films on SPCEs have more electroactive sites than the other films.

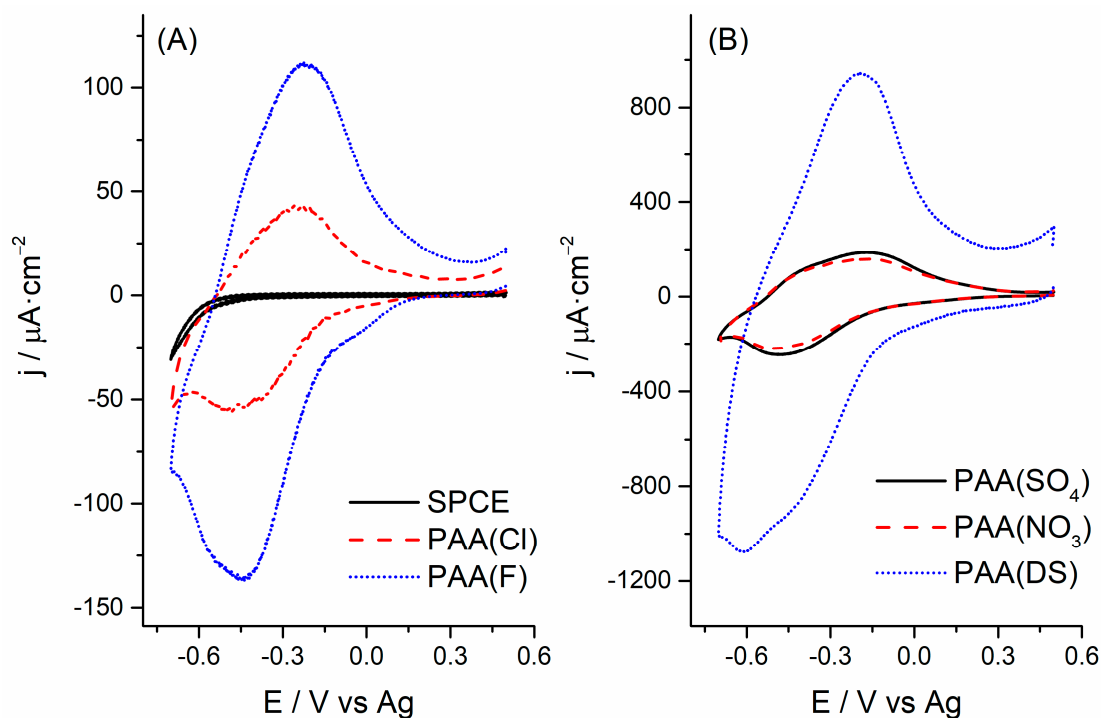


**Figure 2.** Cyclic voltammograms obtained at a bare SPCE (A) and the modified SPCEs with the different PAA films (PAA(Cl) and PAA(F) in (A), and PAA(SO<sub>4</sub>), PAA(NO<sub>3</sub>) and PAA(DS) in (B) at a scan rate of 50 mV·s<sup>-1</sup> in 0.1 M phosphate buffer (pH 7).

### 3.3. Surface Characterization

The electrode surface of the PAA modified SPCEs was characterized by SEM (Figure 3). The surface of a bare SPCE (Figure 3A) shows a similar roughness to SPCEs modified by PAA films electrosynthesized with inorganic monoatomic anions (Figure 3B). As the anion used during the electrosynthesis was more complex, the electrode surface seemed smoother since a larger amount

of PAA was deposited. SPCEs modified by PAA films electrosynthesized with inorganic polyatomic anions (Figure 3C) and with organic polyatomic anions (Figure 3D) significantly covered the working electrode of the SPCE. This tendency is consistent with our discussion on the information extracted from Figure 2.

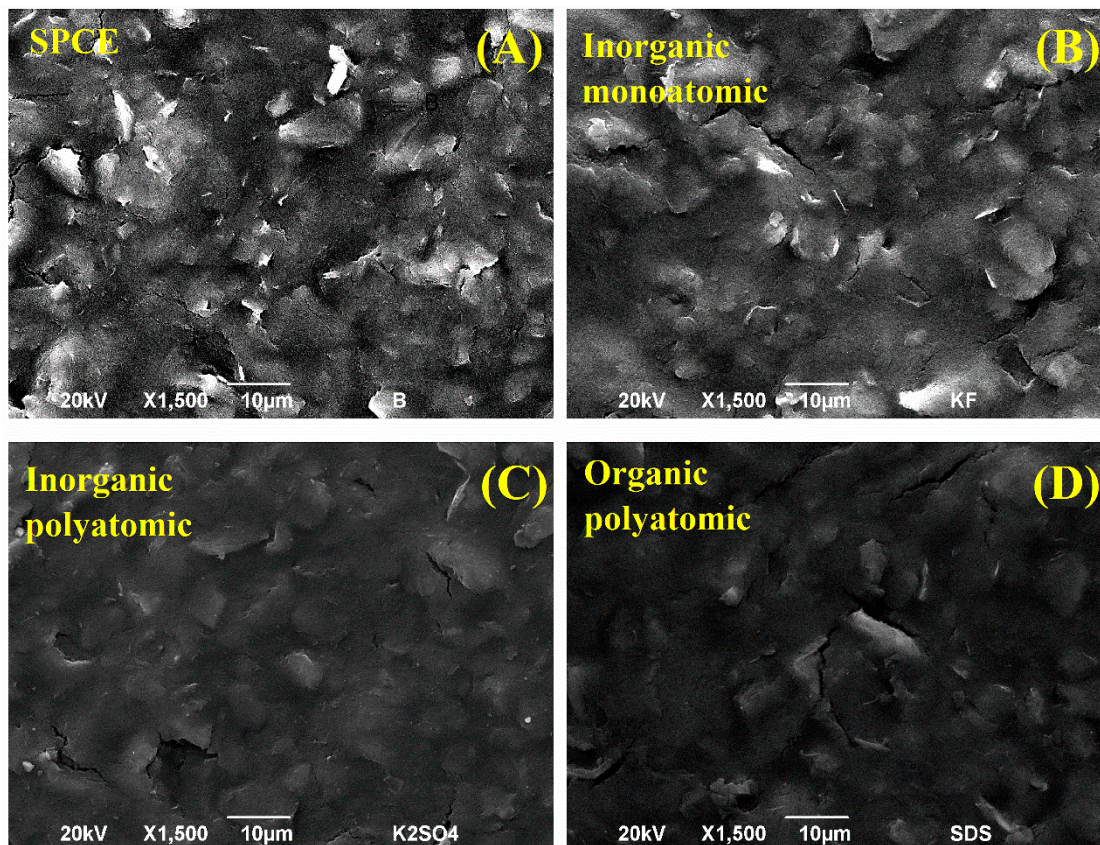


**Figure 3.** SEM images of (A) a bare SPCE and some modified SPCEs by: (B) PAA(F), (C) PAA(SO<sub>4</sub>) and (D) PAA(DS) films. All the images were recorded at 1500× magnification and markers correspond to 10 μm.

### 3.4. Electrochemical Impedance Spectroscopy

Frequency dependent impedance provides the finest information to characterize the surface of electrodes modified with electroactive polymers within the potential range of electroactivity. Figure 4 shows the typical Nyquist plots obtained for a bare SPCE and the SPCEs modified with the different PAA(anion) films in the presence of a redox probe. On the one hand, the electron transfer rate of the ferrocyanide at the electrode | solution interface defines the size of the semicircle or arc portion in the EIS spectrum at relatively high frequencies. On the other hand, the diffusional limiting step of the electrochemical process is shown as the linear portion with a slope of 45° at relatively low frequencies.

Data were fitted to a standard Randel's equivalent circuit depicted in the inset of Figure 4. The uncompensated resistance ( $R_s$ ) describes the electrolyte resistance. The charge transfer resistance ( $R_{ct}$ ) depends on the dielectric and insulating features at the electrode and electrolyte interface. The Warburg impedance ( $W$ ) represents the bulk properties of the electrolyte solution and diffusion features of the redox probe in solution at the lower frequencies. The double layer capacitance was characterized by a constant-phase element (CPE). As observed in Figure 4, a good agreement between the circuit model and the measurement system was obtained. Table 1 shows that the PAA modified SPCEs and the bare SPCE have similar  $R_s$  around 40–50 Ω·cm<sup>2</sup>. CPE increased as the PAA amount on the electrode increased and CPE exponent ( $\alpha$ ) was very close to 1 in all electrodes, indicating a

highly smooth and homogenous electrode surface in accordance with SEM images (Figure 3) [39,40]. The variation of the value of the Warburg impedance suggested that the diffusion process depended on the singular steric hindrance for this process in each PAA film [41].

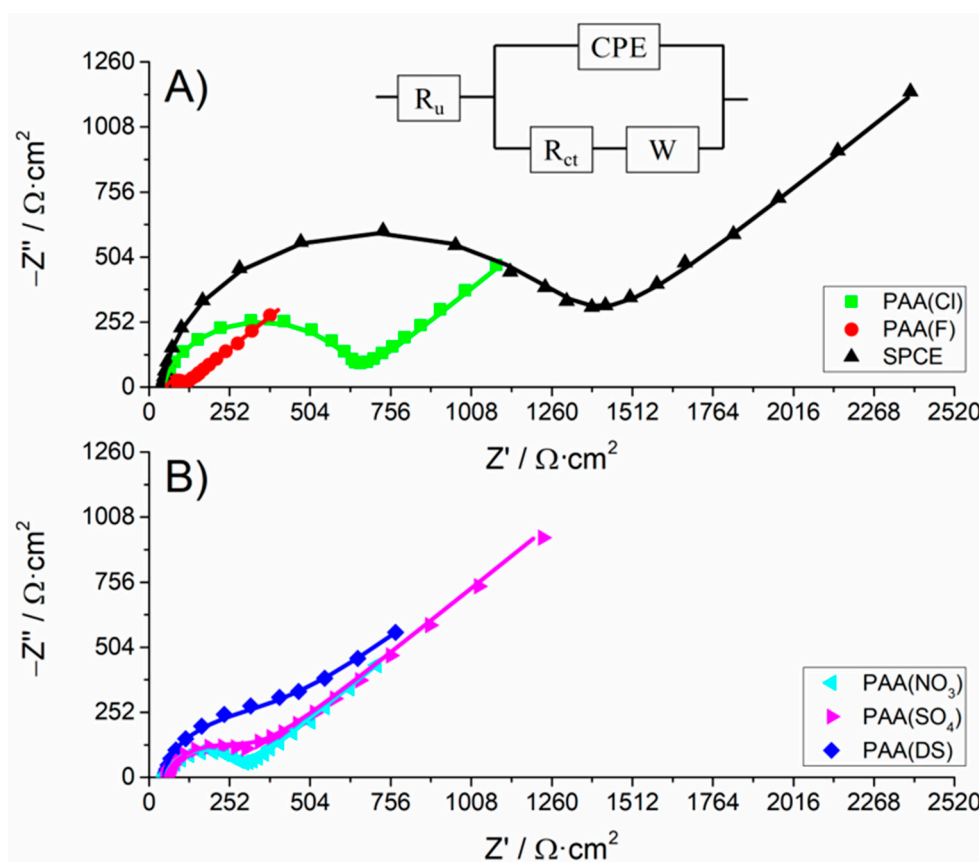


**Figure 4.** Nyquist plots of a bare SPCE (A), black line) and the different PAA(anion) films-modified SPCEs herein prepared, polarized at 0.12 V, measured in 5 mM potassium ferrocyanide and 0.1 M KCl aqueous solution. The perturbation frequency range was from 65 KHz to 10 mHz with an amplitude of 5 mV *rms*. The stabilization time was 60 s. The inset shows the equivalent circuit where  $R_s$  is the uncompensated resistance,  $R_{ct}$  is the charge transfer resistance, CPE is the constant-phase element and W is the Warburg impedance. The points represent experimental data and the lines correspond to the fittings.

**Table 1.** Values of the equivalent circuit elements obtained by fitting the experimental results shown in Figure 4.

Electrode	$R_s \Omega \cdot \text{cm}^2$	CPE $\mu\text{F} \cdot \text{cm}^{-2}$	ff	$R_{ct} \Omega \cdot \text{cm}^2$	$W \Omega \cdot \text{cm}^2 \cdot \text{s}^{-0.5}$
SPCE	42	33	0.9	1233	279
PAA(Cl)	46	29	0.9	585	115
PAA(F)	56	29	1.0	49	75
PAA(NO <sub>3</sub> )	52	56	0.9	227	110
PAA(SO <sub>4</sub> )	52	140	0.9	254	232
PAA(DS)	50	1900	1.0	292	132

Finally,  $R_{ct}$  values clearly proved that PAA films significantly reduced  $R_{ct}$  relative to  $R_{ct}$  of a bare SPCE. It is worth noting the  $R_{ct}$  obtained for the PAA(F) film (around 49  $\Omega \cdot \text{cm}^2$ ) and for the PAA(DS) film (around 292  $\Omega \cdot \text{cm}^2$ ). In the former case, an electrochemical fluorination of PAA cannot be discarded during the PAA electrosynthesis in KF solutions [42], endowing these films with unexpected

properties. The functionalization of PAA films could be an interesting line for further research. In the latter case, it is important to note that  $R_{ct}$  for PAA(DS) was close to other PAA films (PAA(NO<sub>3</sub>) or PAA(SO<sub>4</sub>)), despite PAA(DS) being considered the thickest film in light of the results previously described. This means that the conducting properties of CPs are improved by SDS compared to CPs electrosynthesized in traditional solutions [27,43].

### 3.5. Electrocatalytic Activity

PAA films or derivatives have proved to be good detectors for H<sub>2</sub>O<sub>2</sub> [44,45]. In this work, the electrocatalytic oxidation of H<sub>2</sub>O<sub>2</sub> driven by the PAA films synthesized in the presence of a variety of anions on SPCEs was initially investigated by cyclic voltammetry. Figure 5 shows the cyclic voltammograms obtained in the absence and the presence of hydrogen peroxide for PAA(F) (Figure 5A), PAA(SO<sub>4</sub>) (Figure 5B) and PAA(DS) (Figure 5C). As expected in this kind of films which act as redox mediators [44], H<sub>2</sub>O<sub>2</sub> addition caused the cathodic peak of the PAA(anion) films to increase, while the anodic peak decreased, and in both cases with a significant shift in the respective peak potentials to more cathodic potentials. Simultaneously, a large increment in current at around 0.5 V was also observed. In recent studies [46], the electrocatalytic oxidation of H<sub>2</sub>O<sub>2</sub> by poly(*N*-methylthionine) (or poly(azure C)) has been attributed to the formation of radicals on the electroactive heterocyclic nitrogen atoms in the phenothiazine ring enhancing the electron transfer between the electrode and H<sub>2</sub>O<sub>2</sub>. A similar mechanism may be extrapolated to PAA films because the corresponding monomeric structures of azure A and azure C only differ in a methyl group.

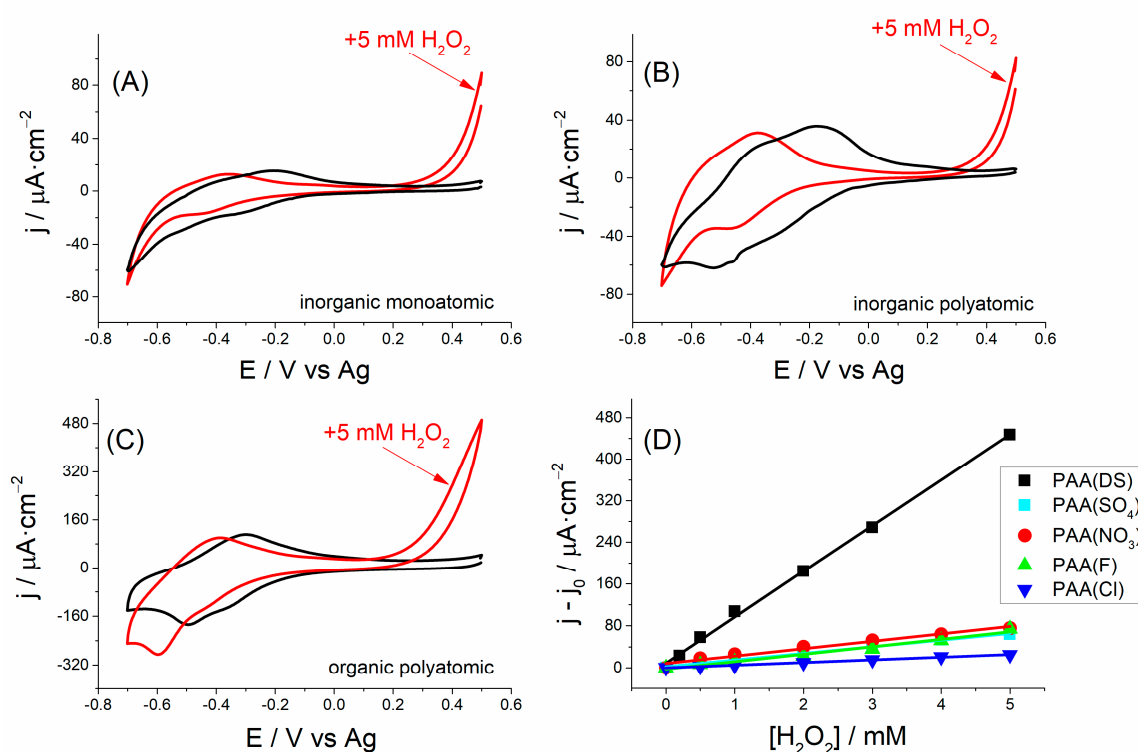
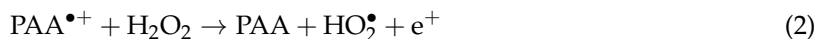


**Figure 5.** Cyclic voltammograms (scan rate: 10 mV·s<sup>-1</sup>, 0.1 M phosphate buffer (pH 7)) of different PAA(anion) films in the absence (black lines) and presence of 5 mM H<sub>2</sub>O<sub>2</sub> (red lines) for PAA(F), PAA(SO<sub>4</sub>) and PAA(DS) films ((A–C), respectively). (D) Current at 0.5 V vs. H<sub>2</sub>O<sub>2</sub> concentration for all modified SPCEs. Error bars correspond to three replicates for each modified electrode.

In our case, the initial state of PAA was assumed completely deprotonated at pH 7 [27]. Then, the polymer would be oxidized to a free radical (Equation (1)) when applied potentials arrived to 0.5 V. Free radicals in phenazine derivatives have been assumed to form in some conditions [47,48]. Cationic



radicals would immediately be reduced by  $\text{H}_2\text{O}_2$ , yielding again the initial state of PAA, and  $\text{HO}_2^\bullet$  (Equation (2)). The  $\text{HO}_2^\bullet$  free radical would end decomposing into  $\text{O}_2$  and  $\text{H}^+$  (Equation (3)).



Focusing our attention around 0.5 V, we observed that the current increment on this zone yielded a greater sensitivity than the cathodic peak current (around  $-0.5$  V) in all modified SPCEs. In particular, we observed that the polymer synthesized in SDS showed the maximum current increase (Figure 5C). In a detailed calibration plot with the addition of different  $\text{H}_2\text{O}_2$  concentrations (Figure 5D), PAA(DS) films showed the best sensitivity among all modified SPCEs.

Based on the best sensing performance obtained at 0.5 V, we tested the potential application of the PAA(DS) films deposited on SPCEs to measure  $\text{H}_2\text{O}_2$  by amperometry. The different  $\text{H}_2\text{O}_2$  concentrations in 0.1 M phosphate buffer (pH 7) were measured on a bare SPCE and a PAA(DS) modified SPCE after polarization of the electrodes at 0.5 V for 600 s. Figure 6 shows the amperometric response to successive additions of  $\text{H}_2\text{O}_2$  for both electrodes. As seen, the bare SPCE showed a poor current signal response to  $\text{H}_2\text{O}_2$  additions. Conversely, the PAA(DS) modified SPCE showed a well-defined step response. The current generated was used to calculate the sensitivity and limit of detection (LOD) of the system (inset of Figure 6). Sensitivity was calculated to be  $72.4 \pm 0.49 \text{ nA} \cdot \mu\text{M}^{-1} \cdot \text{cm}^{-2}$  and the LOD was  $1.43 \pm 0.10 \mu\text{M}$  (estimated at a signal-to-noise ratio of 3). The amperometric response of the same electrode previously used was once again tested after 160 min, and it was kept constant with no significant loss of signal, which indicated the valuable stability of the modified electrode. Sensor repeatability was high with an RSD of 3.4% ( $n = 5$ ). Reproducibility using three different electrodes was 6.2%. The sensor also demonstrated good stability since after 25 measurements of  $10 \mu\text{M}$   $\text{H}_2\text{O}_2$  it maintained 100% of the initial signal. Additionally, it should be mentioned that the linear range was notably wide, from  $5 \mu\text{M}$  to 3 mM (see Figure S2 in the Supplementary Material).

The analytical parameters obtained with our system fell within the range of other non-enzymatic sensors of  $\text{H}_2\text{O}_2$  based on azine derivative polymers, which reached LODs of a micromolar order. Table 2 shows a comparative study of the analytical performance for the non-enzymatic sensing of  $\text{H}_2\text{O}_2$  for different modified electrodes with a variety of conjugated polymers [46,49–55]. As can be seen, sensitivity reached with our system shows an acceptable value, similar to that obtained by other authors. It is important to bear in mind that most modified electrodes shown in Table 2 are based on conventional electrodes, such as glassy carbon (GC). Very few works exist on non-enzymatic hydrogen peroxide sensing using CPs deposited on disposable SPEs. The only sensor using CPs-modified SPEs was in [51], where the authors achieved excellent results, such as good sensitivity and a low LOD. However, the fabrication procedure in this report required a previous chemical step for the synthesis of nanoparticles (NPs), and then the use of piezoelectric inkjet printing techniques to deposit these NPs on the electrode surface. In contrast, the polymerization process to prepare the PAA(DS) modified SPCEs herein proposed is easy and fast, and the only requirement is a very simple electrochemical step using commercial electrodes, which allows the device to be ready for use with no complex manufacturing in just 2 h. Additional advantages of the PAA(DS) modified SPCEs include the excellent benefits of disposable screen-printed electrodes, such as simplicity, low cost, the possibility of using microvolumes and in situ analyses.

In order to test the applicability of this sensor with real samples, interferences from a number of substances were examined. Ethanol, sodium citrate, glucose, caffeine and DHA were added to the cell to obtain final concentrations of 0.1 mM and no response was detected (Figure S3 in Supplementary Material). Furthermore, the signal for  $50 \mu\text{M}$   $\text{H}_2\text{O}_2$  was the same in both the absence and presence of these substances. However, sodium ascorbate was able to affect the amperometric signal (inset of

Figure S3, Supplementary Material). Nevertheless, this interference can be solved by the addition of ascorbate oxidase [56] since the product of the enzymatic process, DHA, does not interfere the signal.

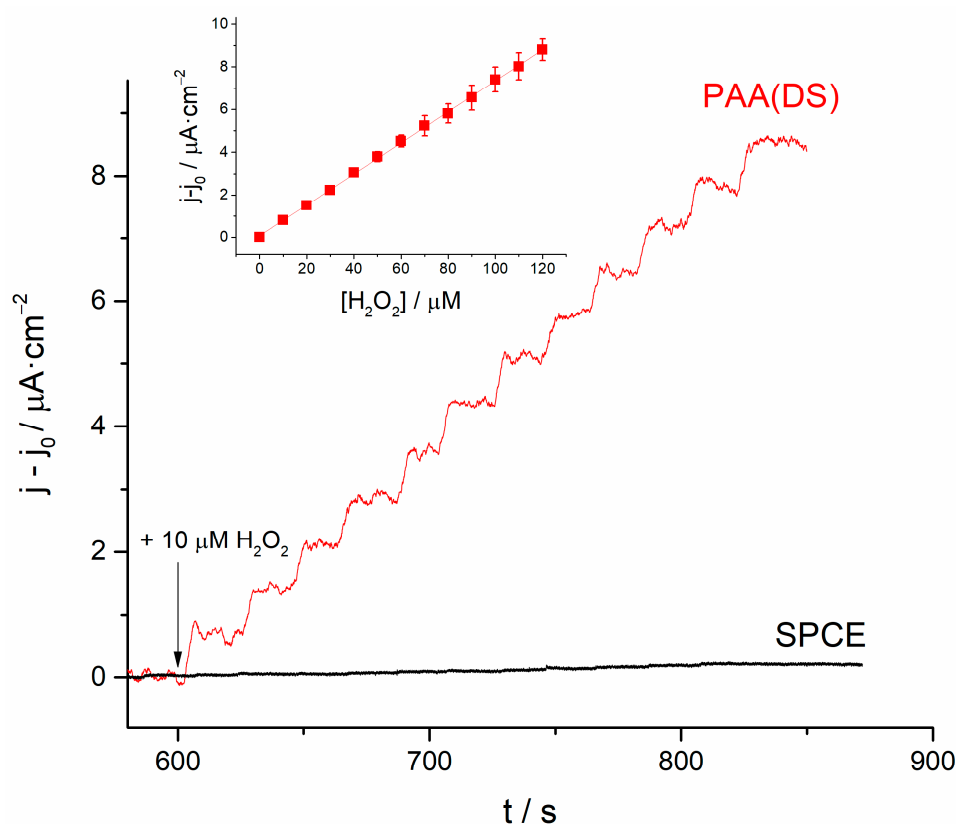


**Figure 6.** Amperometric response of a bare SPCE (black line) and a PAA(DS) | SPCE (red line) upon successive additions of 10  $\mu\text{M}$   $\text{H}_2\text{O}_2$  in phosphate buffer solution (pH 7) at 0.5 V. The inset shows the calibration straight line obtained from the current for the PAA(DS) | SPCE. Error bars are related to the standard deviation of three different measurements.

**Table 2.** Comparison of the electroanalytical parameters used for a variety of electrodes modified with different CPs for the non-enzymatic sensing of  $\text{H}_2\text{O}_2$ .

Electrode <sup>a</sup>	E (V)	Reference Electrode	LOD ( $\mu\text{M}$ )	Sensitivity ( $\text{nA}\cdot\mu\text{M}^{-1}\cdot\text{cm}^{-2}$ )	Reference
Pt foil   PNMTh	0.60	SCE	0.1	2786.0	[46]
GCE   PAA-CS   Cu	-0.40	SCE	0.7	88.9	[49]
PAA-PNR   MWCNTs	-0.25	Ag/AgCl	1.0	10.3	[50]
SPCE   PBNPs	0.00	Ag/AgCl <sup>b</sup>	0.2	762.0	[51]
GCE   PMB-FAD	-0.45	Ag/AgCl	0.1	1109.0	[52]
CF   PEDOT-PNR	-0.36	SCE	80	0.9	[53]
GCE   PTH-Au	-0.10	Ag/AgCl	0.2	14.1	[54]
GCE   PBCB   SWCNT	-0.30	SCE	120.0	58.1	[55]
PAA(DS)   SPCE	0.50	Ag	1.4	72.4	This work

<sup>a</sup> CF: carbon film, CS: chitosan, FAD: flavin adenine dinucleotide, GCE: glassy carbon electrode, MWCNT: multi-walled carbon nanotube, PBCB: poly(brilliant cresyl blue), PBNP: Prussian blue nanoparticles, PEDOT: poly(3,4-ethylenedioxythiophene), PMB: poly(methylene blue), PNMTh: poly(*N*-methylthione), PNR: poly(neutral red), PTH: poly(thionine), SCE: saturated calomel electrode, SWCNT: single-walled carbon nanotubes. <sup>b</sup> This is a pseudo-reference electrode made of conductive ink.

Finally, in order to check the applicability of the PAA(DS) modified SPCEs herein prepared, they were used to determine the  $\text{H}_2\text{O}_2$  concentration in a commercial hair lightener and an antiseptic.

The concentrations calculated by the standard additions method using amperometry were compared to those obtained by a standard spectrophotometric method with xylenol orange (Table 3). The results obtained by these two methods were similar, with a coefficient of variation (% CV) of <1%, which revealed the good precision of PAA(DS) films for H<sub>2</sub>O<sub>2</sub> sensing.

**Table 3.** Hydrogen peroxide found in the commercial samples measured by both the electrochemical and xylenol orange methods.

Sample <sup>a</sup>	Electrochemical Method (M)	Spectrophotometric Method (M)	Recovery (%)
Hair lightener	1.20 ± 0.01	1.19 ± 0.04	100.8
Antiseptic	0.84 ± 0.02	0.85 ± 0.04	98.9

<sup>a</sup> The samples were diluted in phosphate buffer (pH 7) to be measured within the linear range of each analytical method. Three replicates were performed. Values are given as mean ± standard deviation.

#### 4. Conclusions

In this work, PAA films were successfully deposited on disposable SPCEs using different doping anions in the electrosynthesis solution. Of all the anions classified as inorganic monoatomic, inorganic polyatomic and organic polyatomic, dodecyl sulfate anions allowed the synthesis of a PAA film with significantly improved electrochemical properties, despite the film deposited in the presence of dodecyl sulfate substantially covering the working electrode surface. Polymerization in the presence of this surfactant allowed a better electrocatalytic oxidation of H<sub>2</sub>O<sub>2</sub> compared to the same polymer electrosynthesized in the presence of other anions or a bare SPCE. The applicability of the modified electrode as a hydrogen peroxide sensor has been shown, with a linear response for this molecule within the 5 μM to 3 mM range, a 1.43 ± 0.10 μM limit of detection (signal-to-noise ratio of 3) and 72.4 ± 0.49 nA·μM<sup>-1</sup>·cm<sup>-2</sup> sensitivity. In addition, the hydrogen peroxide concentration was measured in real commercial hair lightener and antiseptic samples, with similar results to those obtained by a standard spectrophotometric method. Therefore, the use of PAA(DS) films-modified SPCEs to measure peroxides represents a simple method that avoids long and complex sensor fabrication processes, and one that could be the basis for manufacturing new low-cost sensor electrodes. These results can be extrapolated to the electrodeposition of PAA(DS) films in different kind of electrodes intended for H<sub>2</sub>O<sub>2</sub> electrocatalysis.

**Supplementary Materials:** The following are available online at [www.mdpi.com/2073-4360/10/1/48/s1](http://www.mdpi.com/2073-4360/10/1/48/s1), Figure S1: Polarization curves of 1 mg·mL<sup>-1</sup> azure A in 0.02 M KCl (A) and KNO<sub>3</sub> (B) aqueous solutions at scan rate 10 mV·s<sup>-1</sup> between -0.25 V and 1 V. The voltammetry cycle starts at 0.5 V; Figure S2: Calibration straight line of the PAA(DS) obtained from the amperometric response of such electrode upon successive additions of H<sub>2</sub>O<sub>2</sub> in phosphate buffer solution (pH 7) at 0.5 V. The error bars correspond to standard deviations between three replicates using the same electrode; Figure S3: Amperometry of the influence of certain compounds measured at 0.5 V. 50 μM hydrogen peroxide, 100 μM ethanol, 100 μM sodium citrate, 100 μM glucose, 100 μM caffeine and 100 μM DHA were added to a stirred solution containing phosphate buffer 0.1 M (pH 7). The inset shows the effect of the addition of 50 μM sodium ascorbate compared to the same concentration of hydrogen peroxide.

**Acknowledgments:** This work was supported by the Spanish Ministry of Economy and Competitiveness (MINECO, Spain) [grant numbers BFU2013-44095-P and BFU2016-75609-P (cofunded with FEDER funds, EU)]. BGM is a post-doctoral research fellow of the Youth Employment Initiative (JCCM, Spain, cofunded with ESF funds, EU). The funders played no role in the study design; the collection, analysis or interpretation of data; the writing of the report; the decision to submit the article for publication.

**Author Contributions:** Jerónimo Agrisuelas and María-Isabel González-Sánchez contributed equally to this work. Jerónimo Agrisuelas, María-Isabel González-Sánchez and Edelmira Valero conceived and designed the experiments; Jerónimo Agrisuelas, María-Isabel González-Sánchez and Beatriz Gómez-Monedero performed the experiments; Jerónimo Agrisuelas, María-Isabel González-Sánchez and Beatriz Gómez-Monedero analyzed the data; Jerónimo Agrisuelas, María-Isabel González-Sánchez and Edelmira Valero wrote the paper; Jerónimo Agrisuelas, María-Isabel González-Sánchez, Beatriz Gómez-Monedero and Edelmira Valero revised the manuscript.

**Conflicts of Interest:** The authors declare no conflict of interest.

## References

1. Zhang, Y.; Wilson, G.S. Electrochemical oxidation of H<sub>2</sub>O<sub>2</sub> on Pt and Pt + Ir electrodes in physiological buffer and its applicability to H<sub>2</sub>O<sub>2</sub>-based biosensors. *J. Electroanal. Chem.* **1993**, *345*, 253–271. [[CrossRef](#)]
2. Gonzalez-Sanchez, M.I.; Gonzalez-Macia, L.; Perez-Prior, M.T.; Valero, E.; Hancock, J.; Killard, A.J. Electrochemical detection of extracellular hydrogen peroxide in *Arabidopsis thaliana*: A real-time marker of oxidative stress. *Plant Cell Environ.* **2013**, *36*, 869–878. [[CrossRef](#)] [[PubMed](#)]
3. Agrisuelas, J.; Garcia-Jareño, J.J.; Rivas, P.; Rodriguez-Mellado, J.M.; Vicente, F. Electrochemistry and electrocatalysis of a Pt@poly(neutral red) hybrid nanocomposite. *Electrochim. Acta* **2015**, *171*, 165–175. [[CrossRef](#)]
4. Agrisuelas, J.; Gonzalez-Sanchez, M.-I.; Valero, E. Hydrogen peroxide sensor based on in situ grown Pt nanoparticles from waste screen-printed electrodes. *Sens. Actuators B Chem.* **2017**, *249*, 499–505. [[CrossRef](#)]
5. Miao, P.; Wang, B.; Yin, J.; Chen, X.; Tang, Y. Electrochemical tracking hydrogen peroxide secretion in live cells based on autocatalytic oxidation reaction of silver nanoparticles. *Electrochem. Commun.* **2015**, *53*, 37–40. [[CrossRef](#)]
6. Wang, Y.; Wang, Z.; Rui, Y.; Li, M. Horseradish peroxidase immobilization on carbon nanodots/CoFe layered double hydroxides: Direct electrochemistry and hydrogen peroxide sensing. *Biosens. Bioelectron.* **2015**, *64*, 57–62. [[CrossRef](#)] [[PubMed](#)]
7. Janata, J.; Josowicz, M. Conducting polymers in electronic chemical sensors. *Nat. Mater.* **2003**, *2*, 19–24. [[CrossRef](#)] [[PubMed](#)]
8. Omar, F.S.; Duraisamy, N.; Ramesh, K.; Ramesh, S. Conducting polymer and its composite materials based electrochemical sensor for Nicotinamide Adenine Dinucleotide (NADH). *Biosens. Bioelectron.* **2016**, *79*, 763–775. [[CrossRef](#)] [[PubMed](#)]
9. González-Sánchez, M.I.; Laurenti, M.; Rubio-Retama, J.; Valero, E.; Lopez-Cabarcos, E. Fluorescence Decrease of Conjugated Polymers by the Catalytic Activity of Horseradish Peroxidase and Its Application in Phenolic Compounds Detection. *Biomacromolecules* **2011**, *12*, 1332–1338. [[CrossRef](#)] [[PubMed](#)]
10. González-Sánchez, M.-I.; Laurenti, M.; Rubio-Retama, J.; López-Cabarcos, E.; Valero, E. Searching for the fluorescence quenching mechanism of conjugated polymers by cytochrome c. *Colloids Surf. A Physicochem. Eng. Asp.* **2016**, *510*, 300–308. [[CrossRef](#)]
11. Yano, J.; Kobayashi, M.; Yamasaki, S.; Harima, Y.; Yamashita, K. Mean redox potentials of polyaniline determined by chronocoulometry. *Synth. Met.* **2001**, *119*, 315–316. [[CrossRef](#)]
12. Elmansouri, A.; Outzourhit, A.; Lachkar, A.; Hadik, N.; Abouelaoualim, A.; Achour, M.E.; Oueriagli, A.; Ameziane, E.L. Influence of the counter ion on the properties of poly(o-toluidine) thin films and their Schottky diodes. *Synth. Met.* **2009**, *159*, 292–297. [[CrossRef](#)]
13. Mohamoud, M.A.; Hillman, A.R. The effect of anion identity on the viscoelastic properties of polyaniline films during electrochemical film deposition and redox cycling. *Electrochim. Acta* **2007**, *53*, 1206–1216. [[CrossRef](#)]
14. Vidal, J.-C.; Garcia-Ruiz, E.; Castillo, J.-R. Recent Advances in Electropolymerized Conducting Polymers in Amperometric Biosensors. *Microchim. Acta* **2003**, *143*, 93–111. [[CrossRef](#)]
15. Silk, T.; Hong, Q.; Tamm, J.; Compton, R.G. AFM studies of polypyrrole film surface morphology I. The influence of film thickness and dopant nature. *Synth. Met.* **1998**, *93*, 59–64. [[CrossRef](#)]
16. Windmiller, J.R.; Wang, J. Wearable Electrochemical Sensors and Biosensors: A Review. *Electroanalysis* **2013**, *25*, 29–46. [[CrossRef](#)]
17. Lezi, N.; Economou, A.; Barek, J.; Prodromidis, M. Screen-Printed Disposable Sensors Modified with Bismuth Precursors for Rapid Voltammetric Determination of 3 Ecotoxic Nitrophenols. *Electroanalysis* **2014**, *26*, 766–775. [[CrossRef](#)]
18. Michopoulos, A.; Florou, A.B.; Prodromidis, M.I. Ultrasensitive Determination of Vitamin B12 Using Disposable Graphite Screen-Printed Electrodes and Anodic Adsorptive Voltammetry. *Electroanalysis* **2015**, *27*, 1876–1882. [[CrossRef](#)]
19. González-Sánchez, M.I.; Lee, P.T.; Guy, R.H.; Compton, R.G. In situ detection of salicylate in *Ocimum basilicum* plant leaves via reverse iontophoresis. *Chem. Commun.* **2015**, *51*, 16534–16536. [[CrossRef](#)] [[PubMed](#)]
20. González-Sánchez, M.I.; Valero, E.; Compton, R.G. Iodine mediated electrochemical detection of thiols in plant extracts using platinum screen-printed electrodes. *Sens. Actuators B Chem.* **2016**, *236*, 1–7. [[CrossRef](#)]

21. Karyakin, A.A.; Karyakina, E.E.; Schmidt, H.-L. Electropolymerized Azines: A New Group of Electroactive Polymers. *Electroanalysis* **1999**, *11*, 149–155. [[CrossRef](#)]
22. Agrisuelas, J.; Gabrielli, C.; García-Jareño, J.J.; Gimenez-Romero, D.; Perrot, H.; Vicente, F. Spectroelectrochemical identification of the active sites for protons and anions insertions into poly(Azure A) thin polymer films. *J. Phys. Chem. C* **2007**, *111*, 14230–14237. [[CrossRef](#)]
23. Agrisuelas, J.; Gabrielli, C.; Garcia-Jareno, J.J.; Perrot, H.; Vicente, F. Ionic and Free Solvent Motion in Poly(azure A) Studied by ac-Electrogravimetry. *J. Phys. Chem. C* **2011**, *115*, 11132–11139. [[CrossRef](#)]
24. Gao, Q.; Cui, X.; Yang, F.; Ma, Y.; Yang, X. Preparation of poly(thionine) modified screen-printed carbon electrode and its application to determine NADH in flow injection analysis system. *Biosens. Bioelectron.* **2003**, *19*, 277–282. [[CrossRef](#)]
25. Gao, Q.; Wang, W.D.; Ma, Y.; Yang, X.R. Electrooxidative polymerization of phenothiazine derivatives on screen-printed carbon electrode and its application to determine NADH in flow injection analysis system. *Talanta* **2004**, *62*, 477–482. [[CrossRef](#)] [[PubMed](#)]
26. Sahin, M.; Ayranci, E. Electrooxidation of NADH on Modified Screen-Printed Electrodes: Effects of Conducting Polymer and Nanomaterials. *Electrochim. Acta* **2015**, *166*, 261–270. [[CrossRef](#)]
27. Agrisuelas, J.; González-Sánchez, M.-I.; Valero, E. Electrochemical Properties of Poly(Azure A) Films Synthesized in Sodium Dodecyl Sulfate Solution. *J. Electrochem. Soc.* **2017**, *164*, G1–G9. [[CrossRef](#)]
28. Gay, C.; Collins, J.; Gebicki, J.M. Hydroperoxide Assay with the Ferric-Xylenol Orange Complex. *Anal. Biochem.* **1999**, *273*, 149–155. [[CrossRef](#)] [[PubMed](#)]
29. Bondarenko, A.S.; Ragoisha, G.A. Inverse Problem In Potentiodynamic Electrochemical Impedance. In *Progress in Chemometrics Research*; Pomerantsev, A.L., Ed.; Nova Science Publishers: New York, NY, USA, 2005; pp. 89–102, ISBN 1-59454-257-0.
30. Kamata, K.; Suzuki, T.; Kawai, T.; Iyoda, T. Voltammetric anion recognition by a highly cross-linked polyviologen film. *J. Electroanal. Chem.* **1999**, *473*, 145–155. [[CrossRef](#)]
31. Naoi, K.; Lien, M.; Smyrl, W.H. Quartz Crystal Microbalance Study: Ionic Motion across Conducting Polymers. *J. Electrochem. Soc.* **1991**, *138*, 440–445. [[CrossRef](#)]
32. Ramkumar, R.; Sundaram, M.M. Electrochemical synthesis of polyaniline cross-linked NiMoO<sub>4</sub> nanofibre dendrites for energy storage devices. *New J. Chem.* **2016**, *40*, 7456–7464. [[CrossRef](#)]
33. Shan, D.; Mu, S.L.; Mao, B.W. Detection of intermediate during the electrochemical polymerization of azure B and growth of poly(Azure B) film. *Electroanalysis* **2001**, *13*, 493–498. [[CrossRef](#)]
34. Agrisuelas, J.; Giménez-Romero, D.; García-Jareño, J.J.; Vicente, F. Vis/NIR spectroelectrochemical analysis of poly-(Azure A) on ITO electrode. *Electrochem. Commun.* **2006**, *8*, 549–553. [[CrossRef](#)]
35. Pauliukaite, R.; Brett, C.M.A. Poly(neutral red): Electrosynthesis, Characterization, and Application as a Redox Mediator. *Electroanalysis* **2008**, *20*, 1275–1285. [[CrossRef](#)]
36. Peng, Z.; Guo, L.; Zhang, Z.; Tesche, B.; Wilke, T.; Ogermann, D.; Hu, S.; Kleinermanns, K. Micelle-assisted one-pot synthesis of water-soluble polyaniline-gold composite particles. *Langmuir* **2006**, *22*, 10915–10918. [[CrossRef](#)] [[PubMed](#)]
37. Yang, C.; Zhao, J.; Xu, J.; Hu, C.; Hu, S. A highly sensitive electrochemical method for the determination of Sudan I at polyvinylpyrrolidone modified acetylene black paste electrode based on enhancement effect of sodium dodecyl sulphate. *Int. J. Environ. Anal. Chem.* **2009**, *89*, 233–244. [[CrossRef](#)]
38. Deng, P.; Feng, Y.; Fei, J. A new electrochemical method for the determination of trace molybdenum(VI) using carbon paste electrode modified with sodium dodecyl sulfate. *J. Electroanal. Chem.* **2011**, *661*, 367–373. [[CrossRef](#)]
39. Gabrielli, C.; Takenouti, H.; Haas, O.; Tsukada, A. Impedance investigation of the charge transport in film-modified electrodes. *J. Electroanal. Chem. Interfacial Electrochem.* **1991**, *302*, 59–89. [[CrossRef](#)]
40. Presa, M.J.R.; Tucceri, R.I.; Florit, M.I.; Posadas, D. Constant phase element behavior in the poly(o-toluidine) impedance response. *J. Electroanal. Chem.* **2001**, *502*, 82–90. [[CrossRef](#)]
41. Nowicka, A.M.; Fau, M.; Rapecki, T.; Donten, M. Polypyrrole-Au Nanoparticles Composite as Suitable Platform for DNA Biosensor with Electrochemical Impedance Spectroscopy Detection. *Electrochim. Acta* **2014**, *140*, 65–71. [[CrossRef](#)]
42. Inagi, S.; Fuchigami, T. Electrochemical Post-Functionalization of Conducting Polymers. *Macromol. Rapid Commun.* **2014**, *35*, 854–867. [[CrossRef](#)] [[PubMed](#)]

43. Lin, Y.-C.; Hsu, F.-H.; Wu, T.-M. Enhanced conductivity and thermal stability of conductive polyaniline/graphene composite synthesized by in situ chemical oxidation polymerization with sodium dodecyl sulfate. *Synth. Met.* **2013**, *184*, 29–34. [[CrossRef](#)]
44. Lin, K.C.; Lin, Y.C.; Chen, S.M. Electrocatalytic reaction of hydrogen peroxide and NADH based on poly(neutral red) and FAD hybrid film. *Analyst* **2012**, *137*, 186–194. [[CrossRef](#)] [[PubMed](#)]
45. Baskar, S.; Chang, J.-L.; Zen, J.-M. Simultaneous detection of NADH and H<sub>2</sub>O<sub>2</sub> using flow injection analysis based on a bifunctional poly(thionine)-modified electrode. *Biosens. Bioelectron.* **2012**, *33*, 95–99. [[CrossRef](#)] [[PubMed](#)]
46. Chen, C.; Hong, X.; Xu, T.; Chen, A.; Lu, L.; Gao, Y. Electrocatalytic Oxidation and Determination of Hydrogen Peroxide at Poly(*N*-methylthionine) Electrodes. *J. Electrochem. Soc.* **2015**, *162*, H699–H702. [[CrossRef](#)]
47. Gegiou, D.; Huber, J.R.; Weiss, K. Photochemistry of phenoxazine. Flash-photolytic study. *J. Am. Chem. Soc.* **1970**, *92*, 5058–5062. [[CrossRef](#)]
48. Agrisuelas, J.; Gabrielli, C.; García-Jareño, J.J.; Perrot, H.; Sanchis-Gual, R.; Sel, O.; Vicente, F. Evaluation of the electrochemical anion recognition of NO<sub>3</sub><sup>-</sup>-imprinted poly(Azure A) in mixed solutions by ac-electrogravimetry. *Electrochim. Acta* **2016**, *194*, 292–303. [[CrossRef](#)]
49. Liu, T.; Luo, Y.; Wang, W.; Kong, L.; Zhu, J.; Tan, L. Non-enzymatic detection of hydrogen peroxide based on Fenton-type reaction on poly(azure A)-chitosan/Cu modified electrode. *Electrochim. Acta* **2015**, *182*, 742–750. [[CrossRef](#)]
50. Lin, K.C.; Vilian, A.T.E.; Chen, S.M. Using multi-walled carbon nanotubes to enhance coimmobilization of poly(azure A) and poly(neutral red) for determination of nicotinamide adenine dinucleotide and hydrogen peroxide. *RSC Adv.* **2014**, *4*, 45566–45574. [[CrossRef](#)]
51. Cinti, S.; Arduini, F.; Moscone, D.; Palleschi, G.; Killard, A.J. Development of a Hydrogen Peroxide Sensor Based on Screen-Printed Electrodes Modified with Inkjet-Printed Prussian Blue Nanoparticles. *Sensors* **2014**, *14*, 14222–14234. [[CrossRef](#)] [[PubMed](#)]
52. Lin, K.-C.; Yin, C.-Y.; Chen, S.-M. An electrochemical biosensor for determination of hydrogen peroxide using nanocomposite of poly(methylene blue) and FAD hybrid film. *Sens. Actuators B Chem.* **2011**, *157*, 202–210. [[CrossRef](#)]
53. Gonçalves, A.R.; Ghica, M.E.; Brett, C.M.A. Preparation and characterisation of poly(3,4-ethylenedioxythiophene) and poly(3,4-ethylenedioxythiophene)/poly(neutral red) modified carbon film electrodes, and application as sensors for hydrogen peroxide. *Electrochim. Acta* **2011**, *56*, 3685–3692. [[CrossRef](#)]
54. Han, J.; Ma, J.; Ma, Z. One-step synthesis of poly(thionine)-Au nano-network and nanowires and its application for non-enzyme biosensing of hydrogen peroxide. *Electrochem. Commun.* **2013**, *33*, 47–50. [[CrossRef](#)]
55. Liu, H.-J.; Yang, D.-W.; Liu, H.-H. A hydrogen peroxide sensor based on the nanocomposites of poly(brilliant cresyl blue) and single walled-carbon nanotubes. *Anal. Methods* **2012**, *4*, 1421–1426. [[CrossRef](#)]
56. González-Sánchez, M.I.; Agrisuelas, J.; Valero, E.; Compton, R.G. Measurement of Total Antioxidant Capacity by Electrogenerated Iodine at Disposable Screen Printed Electrodes. *Electroanalysis* **2017**, *29*, 1316–1323. [[CrossRef](#)]

